

Lysinibacillus fusiformis M5 induces increased complexity in Bacillus subtilis 168 colony biofilms via hypoxanthine

Running Title: *L. fusiformis* M5 interaction with *B. subtilis* 168

Gallegos-Monterrosa, Ramses; Kankel, Stefanie; Götze, Sebastian; Barnett, Robert; Stallforth, Pierre; Kovács, Ákos T.

Published in:
Journal of Bacteriology

Link to article, DOI:
[10.1128/JB.00204-17](https://doi.org/10.1128/JB.00204-17)

Publication date:
2017

Document Version
Peer reviewed version

[Link back to DTU Orbit](#)

Citation (APA):

Gallegos-Monterrosa, R., Kankel, S., Götze, S., Barnett, R., Stallforth, P., & Kovács, Á. T. (2017). Lysinibacillus fusiformis M5 induces increased complexity in Bacillus subtilis 168 colony biofilms via hypoxanthine: Running Title: *L. fusiformis* M5 interaction with *B. subtilis* 168 . Journal of Bacteriology, 199(22), [e00204-17]. DOI: 10.1128/JB.00204-17

DTU Library Technical Information Center of Denmark

General rights

Copyright and moral rights for the publications made accessible in the public portal are retained by the authors and/or other copyright owners and it is a condition of accessing publications that users recognise and abide by the legal requirements associated with these rights.

- Users may download and print one copy of any publication from the public portal for the purpose of private study or research.
- You may not further distribute the material or use it for any profit-making activity or commercial gain
- You may freely distribute the URL identifying the publication in the public portal

If you believe that this document breaches copyright please contact us providing details, and we will remove access to the work immediately and investigate your claim.

1 ***Lysinibacillus fusiformis* M5 induces increased complexity in *Bacillus subtilis* 168**
2 **colony biofilms via hypoxanthine**

3

4 Ramses Gallegos-Monterrosa¹, Stefanie Kankel¹, Sebastian Götze², Robert Barnett²,
5 Pierre Stallforth^{2,*}, Ákos T. Kovács^{1,3,*}

6

7 ¹ Terrestrial Biofilms Group, Institute of Microbiology, Friedrich Schiller University Jena,
8 Jena, Germany

9 ² Junior Research Group Chemistry of Microbial Communication, Leibniz Institute for
10 Natural Product Research and Infection Biology, Hans Knöll Institute – HKI, Jena,
11 Germany

12 ³ Department of Biotechnology and Biomedicine, Technical University of Denmark,
13 Denmark

14

15 Running Title: *L. fusiformis* M5 interaction with *B. subtilis* 168

16

17 * Address correspondence to: Ákos T. Kovács <atkovacs@dtu.dk> (on microbiology and
18 strain requests) or Pierre Stallforth <pierre.stallforth@leibniz-hki.de> (on isolation and
19 identification of metabolites)

20 **ABSTRACT**

21 In recent years, biofilms have become a central subject of research in the fields of
22 microbiology, medicine, agriculture, or systems biology amongst others. The
23 sociomicrobiology of multispecies biofilms, however, is still poorly understood. Here, we
24 report a screening system that allowed us to identify soil bacteria, which induce
25 architectural changes in biofilm colonies when cocultured with *B. subtilis*. We identified
26 the soil bacterium *Lysinibacillus fusiformis* M5 as inducer of wrinkle-formation in *B.*
27 *subtilis* colonies mediated by a diffusible signaling molecule. This compound was
28 isolated by bioassay-guided chromatographic fractionation. The elicitor was identified to
29 be the purine hypoxanthine using mass spectrometry and nuclear magnetic resonance
30 (NMR) spectroscopy. We show that the induction of wrinkle formation by hypoxanthine is
31 not dependent on signal recognition by the histidine kinases KinA, KinB, KinC, and KinD,
32 which are generally involved in phosphorylation of the master regulator Spo0A.
33 Likewise, we show that hypoxanthine signaling does not induce the expression of
34 biofilm-matrix related operons *epsA-O* and *tasA-sipW-tapA*. Finally, we demonstrate that
35 the purine permease PbuO, but not PbuG, is necessary for hypoxanthine to induce an
36 increase in wrinkle formation of *B. subtilis* biofilm colonies. Our results suggest that
37 hypoxanthine-stimulated wrinkle development is not due to a direct induction of biofilm-
38 related gene expression, but rather caused by the excess of hypoxanthine within *B.*
39 *subtilis* cells, which may lead to cell stress and death.

40

41 **IMPORTANCE**

42 Biofilms are a bacterial lifestyle with high relevance regarding diverse human activities.
43 Biofilms can be favorable, for instance in crop protection. In nature, biofilms are
44 commonly found as multispecies communities displaying complex social behaviors and
45 characteristics. The study of interspecies interactions will thus lead to a better
46 understanding and use of biofilms as they occur outside laboratory conditions. Here, we
47 present a screening method suitable for the identification of multispecies interactions,
48 and showcase *L. fusiformis* as a soil bacterium that is able to live alongside *B. subtilis*
49 and modify the architecture of its biofilms.

50 **INTRODUCTION**

51 Biofilms are microbial populations formed by cells living in high density communities
52 attached to biotic or abiotic surfaces. These cells are often encased in a matrix of
53 polymeric substances that provide the whole population with an increased resistance
54 against environmental stress (1, 2). Furthermore, these communities exhibit highly
55 complex structural organization and social behavior. Thus, biofilms have become an
56 increasingly studied research subject by microbiologists, especially when it became
57 apparent that this lifestyle is widely spread among bacteria and involved in a multitude of
58 biological processes (3, 4). Although much attention has been given to medically
59 relevant biofilms (5, 6), scientists have also studied biofilms in the context of industrial
60 applications (7), bioremediation (8), and crop protection (9).

61

62 In nature, biofilms rarely occur as single-species populations, but rather as mixed
63 communities of diverse bacteria and other microorganisms. This leads to complex
64 interactions between the different members of the community, usually involving
65 communication networks based on chemical signals (10). Additionally, microorganisms
66 need to sense and efficiently adapt to a wide array of environmental cues in order to
67 efficiently regulate biofilm formation (11).

68

69 *Bacillus subtilis* is a soil-dwelling Gram-positive bacterium that has become a model for
70 biofilm research. On agar plates, *B. subtilis* can form large colonies with remarkably
71 complex architecture, while in liquid medium it forms robust floating biofilms known as
72 pellicles. Both forms of biofilms are characterized by a wrinkled surface, which has been
73 associated to the production of exopolysaccharides, biofilm maturation, and mechanical

74 forces concomitant with an increased population complexity (12–14). Moreover, these
75 biofilms display intricate cell heterogeneity, i.e. some cells become matrix producers,
76 while others either produce exoenzymes to harvest nutrients, or form resistant structures
77 known as spores (15, 16). The development of this population heterogeneity is regulated
78 by a complex gene regulatory network involving various sensing kinases i.e. Kin
79 kinases, DegS, and ComP, and their concomitant response regulators: Spo0A, DegU,
80 and ComA respectively; and other downstream regulators, e.g. SinI and SinR (15, 17,
81 18).

82

83 Biofilms produced by *B. subtilis* are not only a good research model, they are also
84 currently applied in crop protection (19, 20), and spores of this organism are readily
85 commercialized as a biocontrol agent for agriculture. *B. subtilis* is a prolific producer of
86 secondary metabolites and many potent antimicrobial compounds inhibiting both
87 bacteria and fungi have been identified (21–23). In addition, it has also been shown that
88 *B. subtilis* activates biofilm-related gene expression in response to chemicals produced
89 by other bacteria closely related to it, for instance by other members of the *Bacillus*
90 genus (24). Interestingly, the signaling role of the molecules can be independent from
91 other effects of the compounds, as in the case of antimicrobial thiazolyl peptides, which
92 can induce biofilm-matrix production in *B. subtilis* even when separated from their
93 antibiotic activity (25). Moreover, other organisms such as *Pseudomonas protegens*, are
94 able to inhibit cell differentiation and biofilm gene expression in *B. subtilis*, possibly as a
95 competition strategy during root colonization (26).

96

97 *B. subtilis* successfully inhabits a congested and competitive ecological niche (27–29),
98 and it is to be expected that this organism has a finely tuned regulatory network
99 governing community behavior. Therefore, further study of the signaling mechanisms
100 that influence *B. subtilis* biofilm formation may enhance the use of this organism, both in
101 biotechnological applications as well as a research model. However, the identification of
102 signals that induce biofilm formation is a poorly investigated field of study, possibly due
103 to the greater general interest in the removal of biofilms in various medical and industrial
104 settings (5, 30–32). Thus, we have established a co-cultivation-based screening method
105 to identify signaling molecules that promote the development of wrinkles in colony
106 biofilms of *B. subtilis*. Using this system, we identified ecologically relevant soil bacteria
107 that are able to induce the formation of large wrinkles in colony biofilms of *B. subtilis*.
108 The majority of these bacteria are members of the family *Bacillaceae*, to which *B. subtilis*
109 belongs. The strain with the clearest wrinkle-inducing effect was identified as
110 *Lysinibacillus fusiformis* M5. The observed effect on *B. subtilis* is dependent on a
111 diffusible signaling molecule, which was identified as hypoxanthine using bioassay-
112 guided fractionation and subsequent structure elucidation using various spectroscopic
113 and spectrometric methods. The induction of wrinkles by hypoxanthine was not
114 dependent on Kin kinases signal transduction, and the expression levels of operons
115 responsible for the production of biofilm matrix components, *epsA-O* and *tapA-sipW-*
116 *tasA*, remained unaffected. We show that uptake of hypoxanthine by permease PbuO is
117 necessary for the increased induction of wrinkle formation in *B. subtilis* biofilm colonies.
118 We therefore suggest that hypoxanthine induces the formation of wrinkles by introducing
119 a metabolic change in *B. subtilis* cells, rather than by direct stimulation of biofilm-related
120 gene expression.

121 **RESULTS**122 **Screening of soil bacteria that induce structural changes in colonies of *B. subtilis*.**

123 We screened a collection of 242 strains isolated from two distinct soil sampling sites in
124 Mexico, in order to identify bacteria that are able to induce biofilm formation or increased
125 complex colony architecture of *B. subtilis*. Importantly, our assay aimed to discover
126 alterations in biofilm colony architecture that was different from the previously described
127 method that identified soil-derived microbes that induce gene expression related to
128 biofilm formation of *B. subtilis* (24). While some *B. subtilis* strains, such as *B. subtilis*
129 NCIB 3610, easily and spontaneously form biofilms, we used a strain that would form
130 architecturally complex colonies only in the presence of specific inducers or nutrient rich
131 conditions. Thus, even weak biofilm-inducing effects would not be overseen. We used
132 *B. subtilis* 168 (Jena stock), a strain that can only form architecturally complex colonies
133 when grown on glucose-rich medium or exposed to signaling molecules as those
134 present in plant root exudates (33). The strain of *B. subtilis* used for the assay (TB48)
135 carried a $P_{\text{hyperspank}}$ -mKATE reporter fusion in order to facilitate the identification of *B.*
136 *subtilis* from the soil strains in mixed colonies. The reporter strain was mixed in different
137 ratios with the bacterial isolates and allowed to form colonies on 2×SG medium for 72
138 hours. Single strain colonies of *B. subtilis* and the soil-derived isolates were also grown
139 as neighboring colonies under the same conditions, inoculated with a spatial distance of
140 5 mm between each other to examine their interactions. The majority of these
141 interactions resulted in the apparent killing of one strain by the other, producing a colony
142 identical to the pure culture colony of the surviving partner (data not shown). However,
143 36 soil strains were able to grow alongside *B. subtilis*, mainly by creating a colony where
144 the strains segregate in sectors. Interestingly, the *B. subtilis* sectors of these mixed

145 colonies showed an increased architectural complexity by forming large wrinkles and a
146 rugose colony surface, compared to its pure colonies, which remained flat (Fig. 1).
147 Furthermore, when single strain colonies of these soil-derived isolates were grown close
148 to *B. subtilis* colonies, the induction of wrinkle formation could be observed in the areas
149 of the *B. subtilis* colony that are closest to the soil strain, but not in the other regions of
150 the colony (Fig. 1). These results suggest that the aforementioned bacteria produce
151 signals that can induce an increased architectural complexity in *B. subtilis* colony
152 biofilms.

153

154 **Structural changes in *B. subtilis* colonies are induced by diffusible signals**
155 **produced by soil bacteria.**

156 In order to elucidate if the observed induction of wrinkle formation is caused by a
157 diffusible signal molecule or due to direct cell-cell interactions, we designed an assay to
158 test the cell-free supernatants of the selected soil strains. In this assay, we used cotton
159 discs infused with cell-free supernatant to simulate colonies of the tested soil strains.

160 *B. subtilis* was inoculated at a distance of 5 mm next to the cotton discs and allowed to
161 grow for 72 hours. Over this period, the growing colony surrounded the cotton discs,
162 coming into contact with the freely diffusing compounds in the supernatants.

163 Using this assay, we observed that the cell-free supernatants of four bacterial isolates
164 were able to induce efficiently the formation of wrinkles in the adjacent *B. subtilis* colony.
165 Importantly, this phenomenon was observed in the periphery of the cotton discs, but not
166 in the areas of the colony farther away from it (Fig. 2). We note that neither the cell-free
167 supernatant of *B. subtilis* itself, nor the medium used to obtain the supernatants, showed
168 the capacity to induce increased wrinkle formation in *B. subtilis* colonies under our

169 tested conditions (Fig. 2). We concluded that the induction of wrinkle formation was due
170 to a diffusible signaling molecule produced by these soil organisms.
171 Using 16S rRNA locus sequencing, we characterized those soil strains whose
172 supernatant could best stimulate wrinkle formation in *B. subtilis*. The majority of the
173 sequenced strains were found to be members of the same phylogenetic family as *B.*
174 *subtilis*, such as *Bacillus pumilus* or *L. fusiformis*. The only exception was a strain
175 identified as the γ -proteobacterium *Acinetobacter variabilis*.

176

177 **Hypoxanthine identified in the supernatant is responsible for wrinkle induction.**

178 The strongest induction of wrinkle formation (defined as the appearance of tall wrinkles
179 and a rugose colony surface) was observed with the supernatant of the soil derived
180 strain identified as *L. fusiformis* M5. For this reason, we decided to further investigate
181 the respective signaling molecule produced by this bacterium using a wrinkle formation
182 assay. Bio-assay-guided fractionation allowed us to identify a compound from *L.*
183 *fusiformis* M5 that induced a similar phenotype as observed when *B. subtilis* and *L.*
184 *fusiformis* M5 were co-cultured. To this end, supernatant of *L. fusiformis* M5 was
185 lyophilized and fractionated using Sephadex G20 as stationary phase. Each fraction was
186 applied to cotton discs and placed on an agar plate in the vicinity of *B. subtilis*. The
187 fraction that induced wrinkle formation was sub-fractionated by high-performance liquid
188 chromatography (HPLC) using a hypercarb column as stationary phase. Repeating this
189 procedure led to the isolation of a homogeneous compound whose structure was
190 subsequently elucidated via a combination of nuclear magnetic resonance (NMR)
191 spectroscopy and high-resolution mass spectrometry (HR-MS). Finally, hypoxanthine
192 was identified as the inducer of wrinkle formation (Fig. 3). We further validated our

193 findings using commercial hypoxanthine, which showed the same retention time as the
194 isolated hypoxanthine (Fig. 3).

195 We used the colony wrinkle formation assay to test if hypoxanthine (as a 25 mM solution
196 in 0.05 N NaOH) alone can induce the formation of wrinkles in *B. subtilis* colony biofilms.

197 In addition, guanine and xanthine were also tested using this methodology, since these
198 purines can be found in the same metabolic pathways as hypoxanthine in *B. subtilis*. We
199 found that hypoxanthine and guanine were able to induce the formation of tall wrinkles in
200 *B. subtilis* colonies, while xanthine could not (Fig. 4a). Interestingly, guanine can be
201 deaminated during purine catabolism to produce hypoxanthine, which can then be
202 oxidized to produce xanthine (Fig. 4b). These results suggest that a metabolite derived
203 from guanine or hypoxanthine, but not xanthine, may be responsible for the observed
204 formation of wrinkles.

205

206 **Hypoxanthine signaling is not mediated by the activity of individual Kin kinases.**

207 In *B. subtilis*, the transcriptional regulator Spo0A controls the expression of several
208 biofilm-related operons, including those responsible for the production of the
209 exopolysaccharide and protein components of the biofilm matrix (*epsA-O* and *tapA-
sipW-tasA*, respectively) (17). Five sensor kinases (KinA, KinB, KinC, KinD, and KinE)
210 have been identified in *B. subtilis*, and four of them (KinA-D) are known to activate
211 Spo0A via a phosphorelay depending on environmental signals (11, 15, 34). We wanted
212 to determine if any of these kinases is involved in hypoxanthine-mediated induction of
213 wrinkles. Therefore, we compared the effect that the supernatant of *L. fusiformis* M5 has
214 on kinase-mutant strains of *B. subtilis* using the colony wrinkle formation assay. We
215 expected that, should one of these kinases be responsible for sensing hypoxanthine, the
216

217 corresponding mutant strain would no longer show increased induction of wrinkle
218 formation. Interestingly, all the mutant strains were still able to develop highly wrinkled
219 colonies when exposed to the supernatant, when compared to the corresponding
220 colonies exposed to 2×SG medium (Fig. 5). This result suggests that hypoxanthine-
221 mediated induction of increased architectural complexity is not mediated by the
222 activation of Spo0A via a single Kin kinase. We note that more than one Kin kinase
223 could be responsible for detecting hypoxanthine, in which case the deletion of a single
224 *kin* kinase gene would not prevent *B. subtilis* to form wrinkled colonies when exposed to
225 hypoxanthine.

226

227 **Expression levels of genes responsible for biofilm matrix production are not**
228 **affected by hypoxanthine signaling.**

229 The *epsA-O* and *tapA-sipW-tasA* operons are related to the production of the
230 exopolysaccharide and protein components of the *B. subtilis* biofilm matrix, respectively.
231 Changes in the expression levels of these operons are associated to a maturing
232 biofilm, and show spatiotemporal variation during its development (16, 35, 36).
233 To further examine if biofilm matrix-related genes are involved in the induction of
234 wrinkles by hypoxanthine, we monitored the expression of $P_{epsA-gfp}$ and $P_{tapA-gfp}$
235 fluorescent reporter fusions in colonies of *B. subtilis* using the colony wrinkle formation
236 assay. Fluorescence emission was examined only in the sections of the colonies directly
237 adjacent to the cotton discs at 3 time points: (i) when *B. subtilis* has encircled the discs
238 (40 hours), (ii) when the colony started to expand from the disc and showed the onset of
239 wrinkle formation (50 hours), and (iii) when the colony has developed wrinkles and
240 expanded (65 hours). The examined strains also carried a $P_{hyperspank-mKATE}$ reporter

241 fusion to adjust for colony growth. Under these conditions, the expression from P_{epsA} and
242 P_{tapA} in these colonies showed no statistical differences when exposed to cotton discs
243 infused with 2×SG medium or supernatant of *B. subtilis*, as compared to those infused
244 with supernatant of *L. fusiformis* M5 (one-way ANOVA: $P < 0.05$, $n = 4-8$ independent
245 colonies) (Fig. 6).

246 We decided to further test if the products of the *epsA-O* and *tapA-sipW-tasA* operons
247 are necessary for the observed development of wrinkles. We used the wrinkle formation
248 assay to test the effect of the supernatant of *L. fusiformis* M5 on mutant strains of *B.*
249 *subtilis* that are unable to produce the exopolysaccharide ($\Delta epsA-O$) or protein ($\Delta tasA$)
250 matrix component. After 72 hours of incubation, the tested *B. subtilis* strains expanded
251 and surrounded the infused cotton discs, but were unable to develop wrinkles and
252 showed a flat and mucoid colony surface (Fig. 7).

253 Taken together, these results suggest that the increased colony wrinkle formation
254 induced by hypoxanthine is not directly associated with a large increase in expression
255 from the biofilm matrix operons; however, the production of a biofilm matrix is necessary
256 for the development of wrinkles.

257

258 **Cell death correlates with wrinkle formation.**

259 It has been shown previously that localized cell death can be a trigger for wrinkle
260 formation in biofilm colonies. This happens as a consequence of mechanical forces
261 converging on zones of cell death, which lead to a buckling of the biofilm and the rise of
262 tall wrinkles (13). Based on our previous results, we hypothesized that hypoxanthine, or
263 a metabolite formed during its catabolism, may cause cell death in *B. subtilis*. This would
264 produce mechanical stress in the developing biofilm and lead to buckling and wrinkle

265 formation. Thus, we used Sytox Green to assess the distribution of dead cells in the
266 colony wrinkle formation assay. Sytox Green is a commercially available fluorescent
267 nucleic acid stain that has been established as a reporter of cell death for bacteria (37).
268 For this assay, we used a *B. subtilis* strain that carries a $P_{hyperspank}$ -mKATE reporter
269 fusion (TB48) in order to facilitate the identification of *B. subtilis* cells that are
270 metabolically active from those that are readily stained by Sytox Green. After 72 hours of
271 incubation, we examined thin cross-sections of colonies that were exposed to 2×SG
272 medium or supernatant from *L. fusiformis* M5. The examined cross-sections
273 corresponded to areas of the colonies adjacent to the cotton discs (Fig. 8a and f). We
274 observed that cell death is localized at the bottom of the biofilm, both on those exposed
275 to 2×SG medium or *L. fusiformis* M5 supernatant (Fig. 8). However, in the cross-sections
276 obtained from the flat colonies of *B. subtilis* exposed to 2×SG medium, the dead cells
277 appear as thin layer of similar width along the length of the cross-section (Fig. 8b-e). In
278 contrast, the cross sections from wrinkled colonies exposed to *L. fusiformis* M5
279 supernatant revealed aggregates of dead cells that correlate with the wrinkles seen
280 through the colony (Fig. 8g-j). Furthermore, we compared the average green
281 fluorescence of the colony cross-sections (produced by cells stained with Sytox Green)
282 with their own red fluorescence (produced by cells expressing the $P_{hyperspank}$ -mKATE
283 reporter fusion). We found that the average ratios of green/red fluorescence were
284 significantly higher in the cross-sections of colonies exposed to *L. fusiformis* M5
285 supernatant ($0.69 \text{ AU} \pm 0.10$ (standard deviation)), than those of cross-sections from
286 colonies exposed to 2×SG medium ($0.33 \text{ AU} \pm 0.02$ (standard deviation)) (one-way
287 ANOVA: $P > 0.05$, $n = 3$ cross-sections from independent colonies). These results confirm

288 that the formation of wrinkles is facilitated by cell death, a phenomenon observed in the
289 presence of the *L. fusiformis* M5 supernatant.

290

291 **The permease PbuO is necessary for hypoxanthine-induced development of**
292 **wrinkles.**

293 We hypothesized that the observed induction of wrinkle formation may be due to
294 metabolic effects on *B. subtilis* cells derived from an excess of available hypoxanthine
295 provided by the culture supernatant of *L. fusiformis* M5, rather than to direct signal-
296 dependent expression of biofilm-related genes. In this case, hypoxanthine alone would
297 be sufficient to induce increased wrinkle formation, and its uptake by *B. subtilis* would be
298 necessary for this phenomenon.

299 Using the colony wrinkle formation assay, we observed that different concentrations of
300 hypoxanthine (as solution in 0.05 N NaOH) were able to induce the formation of wrinkles
301 in *B. subtilis* colonies as efficiently as the supernatant of *L. fusiformis* M5. To test
302 whether hypoxanthine internalization is required for the observed wrinkle induction in *B.*
303 *subtilis*, we analyzed mutant strains of *B. subtilis* that lack *pbuG* or *pbuO*. PbuG is a
304 previously described hypoxanthine/guanine permease (38), while PbuO is a protein
305 paralogous to PbuG annotated as a putative purine permease (see SubtiWiki:
306 <http://subtiwiki.uni-goettingen.de/index.php>) (39). The hypoxanthine inducing effect
307 disappeared when *pbuO* alone, or in combination with *pbuG*, was deleted (Fig. 9).
308 These final results demonstrated that hypoxanthine uptake is important for induction of
309 wrinkle formation and PbuO is mainly responsible for the observed effect under our
310 experimental conditions.

311 **DISCUSSION**

312 In this work, we identified a chemical sensing mechanism between *B. subtilis* and other
313 soil bacteria that promotes architectural complexity in colony biofilms. We devised a
314 screening system that allowed us to analyze a collection of soil bacteria, selecting those
315 that could form stable multispecies communities with *B. subtilis*. Using this screening
316 system, we identified *L. fusiformis* M5 as a bacterium capable of inducing an increase of
317 colony wrinkle formation in *B. subtilis* via hypoxanthine as chemical cue.

318

319 Hypoxanthine is a purine that plays an important role in the pentose phosphate salvage
320 pathway, which is a mechanism for cells to interconvert nucleosides and nucleobases
321 according to their metabolic needs (40, 41). In *B. subtilis*, hypoxanthine is particularly
322 relevant in this pathway because it can be taken up by cells and used as a substrate by
323 phosphoribosyl-transferases in order to produce inosine monophosphate (IMP), which in
324 turn is converted to adenosine monophosphate or guanine monophosphate (38) (also
325 see SubtiWiki Pathways: [http://subtiwiki.uni-](http://subtiwiki.uni-goettingen.de/apps/pathway.php?pathway=2)
326 [goettingen.de/apps/pathway.php?pathway=2](http://subtiwiki.uni-goettingen.de/apps/pathway.php?pathway=2)) (39). The role of hypoxanthine in
327 eukaryotic cell metabolism has been extensively investigated. In humans, it has been
328 studied in the context of diseases such as gout, Lesch–Nyhan disease, and endothelial
329 cell injury of cardiovascular diseases. Although these conditions have different etiologies
330 and clinical evolution, they have in common an excessive accumulation of hypoxanthine
331 and uric acid, whose catabolism leads to oxidative-stress-induced apoptosis (42–44). In
332 bacteria, hypoxanthine has been mainly studied in relation to DNA damage and
333 mutagenesis due to spontaneous deamination of adenine, which yields hypoxanthine
334 and leads to AT-to-GC transitions after DNA replication (45). In *B. subtilis*, hypoxanthine

335 has been studied both related to purine metabolism (38), and DNA damage and repair
336 (46). To the best of our knowledge, this is the first time that hypoxanthine has been
337 reported as a mediator of interactions in *B. subtilis* biofilms.

338

339 *L. fusiformis* is a free-living bacterium that can be isolated from soil and has been
340 studied due to its production of interesting secondary metabolites and bioremediation
341 potential (47–49). Here, we have identified a strain of *L. fusiformis* able to produce and
342 excrete hypoxanthine in sufficient levels to induce the formation of wrinkles in biofilm
343 colonies of *B. subtilis*. We found no evidence that this phenomenon is dependent on the
344 signal transduction of a single Kin kinase (Fig. 5), and the expression levels of the
345 matrix-component-related operons *epsA-O* and *tapA-sipW-tasA* remained equal when *B.*
346 *subtilis* was exposed to the supernatant of *L. fusiformis* M5 (Fig. 6). Importantly, we
347 cannot discard the possibility of changes in the expression of other genes. For example,
348 changes in the expression of motility-related genes might be responsible for the
349 apparent differences in colony expansion observed in our wrinkle formation assays.
350 Another possibility is that an alternative exopolysaccharide biosynthetic pathway could
351 be affected. Recently, *ydaJKLMN* was reported as a new operon important for the
352 production of a so far unidentified exopolysaccharide in *B. subtilis* (50). However,
353 overexpression of the *ydaK-N* operon under a xylose-inducible promoter could promote
354 wrinkle formation in a Δ *epsH* mutant strain (50), while the presence of the *eps* operon is
355 essential for the induction of wrinkle development in the presence of hypoxanthine.
356 Therefore, it seems unlikely that hypoxanthine-induced wrinkle formation would proceed
357 by directly inducing the production of an alternative exopolysaccharide. In contrast, we
358 could detect the presence of dead cells with Sytox Green at the site of wrinkle formation

359 (Fig. 8). Additionally, a knock-out mutant of the hypoxanthine/guanine permease PbuO
360 lost the ability to form wrinkled colonies; specifically, a $\Delta pbuG$ mutant strain showed
361 slightly reduced or similar wrinkle formation as *B. subtilis* 168, while a $\Delta pbuO$ strain
362 completely lost the ability to form wrinkled colonies when exposed to hypoxanthine.
363 Based on these results, we suggest that hypoxanthine induces the formation of wrinkles
364 in colony biofilms of *B. subtilis* not by inducing the expression of biofilm-related genes,
365 but rather by metabolic effects derived from the excess of available hypoxanthine. In this
366 regard, we note that an excess of hypoxanthine can cause oxidative stress and cell
367 death in eukaryotic cells by increasing the formation of reactive oxygen species when
368 hypoxanthine is metabolized to urate (42, 43). A similar catabolic pathway could be
369 followed by hypoxanthine in *B. subtilis*, which possesses multiple hypoxanthine/xanthine
370 oxidases known as PucA, B, C, D and E (see SubtiWiki Pathways:
371 <http://www.subtiwiki.uni-goettingen.de/apps/pathway.php?pathway=41>) (39).
372 Additionally, it has been shown that localized cell death can lead to the formation of
373 wrinkles in colonies of *B. subtilis* by providing an outlet for compressive mechanical
374 forces that buckle the biofilm and promote the appearance of wrinkles (13). Thus, we
375 hypothesize that the hypoxanthine provided by *L. fusiformis* induces oxidative stress and
376 cell death in *B. subtilis*, which leads to the formation of wrinkles as a mechanical
377 consequence. This is in accordance with the fact that the observed development of
378 wrinkles only occurs in the interaction zone between colonies of these organisms (Fig.
379 1), or in the proximity of the cotton discs during our colony wrinkle formation assays
380 (Figs. 5 and 9). This development of wrinkles does not happen in the rest of the *B.*
381 *subtilis* colony, presumably due to a lower concentration of diffused hypoxanthine.
382 Importantly, this induction of increased wrinkle formation in *B. subtilis* would therefore be

383 a consequence of regular metabolic processes of *L. fusiformis*, rather than a canonical
384 signaling mechanism intended to elicit a response in the receiver. Regarding
385 hypoxanthine production by *L. fusiformis* M5, we have previously sequenced this strain,
386 finding genes homologous to those known in other organisms to be responsible for
387 hypoxanthine synthesis and export (51), although more research is needed to establish
388 its production yield. However, we note that hypoxanthine can be produced by
389 spontaneous deamination of adenine, such as that present in the surroundings of
390 decaying cells (52). Unfortunately, our efforts to transform *L. fusiformis* M5 failed,
391 preventing us to construct mutants with altered hypoxanthine production.

392

393 In recent years, biofilm research has grown from an incipient field to a major area of
394 microbiological interest. Due to the high cell density of biofilms, social interactions are an
395 inherent characteristic of these microbial populations, regardless of whether they are
396 formed as single or multi-species communities (10, 28, 53, 54). The interactions
397 between the organisms forming a biofilm are therefore an important aspect of this
398 research field, since they shape the development of these communities, be it by
399 intraspecies signaling, interspecies communications, or chemical cues derived from the
400 metabolism of community members, such as the case presented here. Further study of
401 the sociomicrobiology of biofilms will lead to an increased understanding of these
402 communities as they form in nature, better enabling us to eliminate them when they are
403 noxious to human activities, or to promote them when needed for biotechnological
404 applications.

405 **MATERIAL AND METHODS**

406 **Strains, media, and general culture conditions.**

407 All strains used in this study are listed in Table 1. When fresh cultures were needed,
408 these strains were pre-grown overnight in Lysogeny broth medium (LB-Lennox, Carl
409 Roth; 10 g L⁻¹ tryptone, 5 g L⁻¹ yeast extract, and 5 g L⁻¹ NaCl) at 37°C and shaken at
410 225 r.p.m. LB medium was used for all *B. subtilis* and *Escherichia coli* transformations,
411 and to screen soil samples. 2×SG medium (16 g L⁻¹ nutrient broth (Difco), 2 g L⁻¹ KCl,
412 0.5 g L⁻¹ MgSO₄·7H₂O, 1 mM Ca(NO₃)₂, 0.1 mM MnCl₂·4H₂O, 1 μM FeSO₄, and 0.1%
413 glucose) (55) was used to grow cultures intended for supernatant production. This
414 medium was also used for all strain interaction assays and wrinkle-induction assays.
415 Tryptone Soya broth (CASO-Bouillon, AppliChem; 2.5 g L⁻¹ glucose, 5 g L⁻¹ NaCl, 2.5 g
416 L⁻¹ buffers (pH 7.3), 3 g L⁻¹ soya peptone, and 17 g L⁻¹ tryptone) was used for screening
417 soil samples. GCHE medium (1% glucose, 0.2% glutamate, 100mM potassium
418 phosphate buffer (pH: 7), 3 mM trisodium citrate, 3 mM MgSO₄, 22 mg L⁻¹ ferric
419 ammonium citrate, 50 mg L⁻¹ L-tryptophan, and 0.1% casein hydrolysate) was used to
420 induce natural competence in *B. subtilis* (56). Our developed Gallegos Rich medium was
421 used to grow *Lactococcus lactis* MG1363, in order to purify pMH66: 21 g L⁻¹ tryptone, 5
422 g L⁻¹ yeast extract, 8.3 g L⁻¹ NaCl, 3 g L⁻¹ soya peptone, 2.6 g L⁻¹ glucose, and 2.5 g L⁻¹
423 MgSO₄·7H₂O. Overnight cultures of *L. lactis* were incubated at 30°C without shaking.
424 Media were supplemented with Bacto agar 1.5 % when solid plates were needed.
425 Antibiotics were used at the following final concentrations: kanamycin, 10 μg mL⁻¹;
426 chloramphenicol, 5 μg mL⁻¹; erythromycin-lincomycin, 0.5 μg mL⁻¹ and 12.5 μg mL⁻¹
427 respectively; ampicillin, 100 μg mL⁻¹; spectinomycin, 100 μg mL⁻¹; tetracycline, 10 μg
428 mL⁻¹. Specific growth conditions are described in the corresponding methods section.

429

430 Importantly, all 2×SG plates used in this study were prepared with 25 mL of medium,
431 and dried for a minimum of 20 minutes before use. Insufficient drying resulted in
432 excessive colony expansion without development of architecturally complex colonies. To
433 dry the plates, they were first allowed to solidify at room temperature for 1 hour,
434 afterwards, they were kept completely open in a laminar flow sterile bench for the
435 duration of the drying period. These drying conditions were followed for all assays that
436 examined changes in colony architecture.

437

438 **Strain construction.**

439 All *B. subtilis* strains generated in this work were obtained via natural competence
440 transformation (56) using genomic or plasmid DNA from donor strains as indicated in
441 Table 1. Briefly, overnight cultures of the receiver strains were diluted to a 1:50 ratio with
442 GCHE medium, these cultures were incubated at 37°C for 4 h with shaking at 225 r.p.m.
443 After this incubation period, 5–10 µg of genomic or plasmid DNA were mixed with 500
444 µL of competent cells and further incubated for 2h before plating on LB plates added
445 with selection antibiotics. Strain TB822 was obtained by using the Cre recombinase
446 expressed from plasmid pMH66 to eliminate the Erm^R cassette of TB813, and
447 subsequently curating pMH66 via thermal loss of the plasmid (57). Briefly, TB813 was
448 transformed with 10 µg of pMH66, selecting transformants via incubation at 37°C on LB
449 plates added with tetracycline. Candidates were then screened for their capacity to grow
450 at 37°C on LB plates added with macrolide antibiotics (erythromycin-lincomycin), those
451 that were not able to grow were further incubated on LB plates at 43°C for 18 h to induce

452 the loss of pMH66. Candidates that were then unable to grow at 37°C on LB plates
453 added with tetracycline were considered to have lost pMH66.
454 Successful construction of all used strains and plasmids was validated via PCR and
455 restriction pattern analysis using standard molecular biology techniques, and by the lack
456 of amylase activity on 1% starch LB plates (58) and emission of red fluorescence. All
457 PCR primers used in this study are listed in Table 2. Primer pairs were used to amplify
458 the indicated loci (see Table 2) in order to confirm the proper mutation of the
459 corresponding gene. To confirm the correct construction of strains TB869 and TB870,
460 primer oGFPprev2 was used in combination with oRGM38 (for *sacA::P_{tapA}-gfp*) or
461 oRGM40 (for *sacA::P_{epsA}-gfp*).

462

463 **Isolation of bacteria from soil samples.**

464 Two independent Mexican soil samples were screened to isolate bacteria able to grow
465 on LB or tryptone soya broth media. The first sample was collected from Tepoztlán,
466 Morelos (18° 59' 7" N, 99° 5' 59" W), a humid and verdant region of central Mexico. The
467 second sample was collected from Tehuacán, Puebla (18° 25' 47.71" N, 97° 27' 58.1"
468 W), a semidesertic dry region in east central Mexico. Both samples were collected with a
469 clean metal spatula 5 cm below surface level, and at 15 to 20 cm of the roots of local
470 trees.

471

472 1 g of each soil sample was suspended in 9 mL of a sterile 0.85% NaCl solution, and 50
473 μ L of Tween 80 were added. The resulting suspensions were vortexed for 5 minutes at
474 maximum speed. The bigger soil particles were allowed to sediment by keeping the
475 suspensions still for 10 minutes. The supernatants were then diluted with sterile 0.85%

476 NaCl to 1:1000, 1:10 000 and 1:100 000 ratios. 50 and 100 μ L of these dilutions were
477 spread on LB and tryptone soya broth agar plates. These plates were incubated at 30°C
478 for a maximum of 5 days. Bacterial colonies that grew during the incubation period were
479 further isolated by cross-streaking them on LB or tryptone soya broth plates and
480 incubating them at 30°C for 48 hours. Single isolated colonies obtained from this
481 secondary cultivation were used to prepare liquid cultures on 3 mL of LB media. These
482 cultures were incubated at 30°C with shaking for a maximum of 48 hours. Bacteria that
483 grew efficiently during this incubation period were used to prepare glycerol stock
484 solutions (20% v/v) and stored at -80°C for further use. In total, 242 soil strains were
485 obtained and subsequently tested.

486

487 **Soil strains interaction screening.**

488 Overnight liquid cultures of *B. subtilis* strain TB48 and the obtained soil strains were
489 adjusted to OD₆₀₀ 0.2 using LB medium. These diluted cultures were then mixed in 1:1,
490 10:1, and 1:10 ratios, and 2 μ L of the mixed and pure cultures were inoculated on 2×SG
491 plates. For neighbor colonies interaction assay, 2 μ L of the pure cultures were
492 inoculated at a distance of 5 mm from each other. Plates were incubated at 30°C for 72
493 h. The obtained colonies were used for microscopy analysis without further treatment.

494

495 **Identification of soil strains.**

496 Genomic DNA of selected soil strains was extracted with the GeneMATRIX Bacterial
497 and Yeast Genomic DNA Purification Kit, according to the manufacturer's instructions
498 (EURx, Poland). This DNA was used to PCR amplify a fragment of the 16S rRNA gene
499 using primers 27F and 1492R (59). Amplicons were purified with the High Pure PCR

500 Product Purification Kit according to the manufacturer's instructions (Roche Diagnostics,
501 Switzerland) and sequenced with primers 27F and 1492R (GATC Biotech, Germany).
502 Sequencing results were then compared with sequences in the National Center for
503 Biotechnology Information (16S ribosomal RNA Bacteria and Archaea database) using
504 the BLASTn algorithm (60). Soil strains' identities were established using minimum
505 query coverage of 98% and minimum identity values of 99%.

506

507 **Purification and treatment conditions of soil strain supernatant.**

508 To obtain cell-free supernatants of selected soil strains, 10 mL cultures on 2×SG
509 medium of the corresponding strains were incubated at 30°C for 24 hours with shaking
510 at 100 r.p.m. These cultures were then centrifuged at 7000 r.c.f. for 15 min. The
511 supernatants were collected and filter-sterilized using a 0.22 µm pore-size filter (Carl
512 Roth, Germany).

513

514 **Colony wrinkle formation assay.**

515 We developed the following assay to assess the effect that the supernatants of soil
516 strains, and compound solutions, may have upon the architectural complexity of *B.*
517 *subtilis* colony biofilms. Sterile 12 mm-diameter cotton discs were placed on 90 mm-
518 diameter 2×SG agar plates, in such a way that there is a maximum amount of available
519 space among the discs themselves and between the discs and the border of the plates.
520 3 cotton discs were used per plate. 50 µL of the tested supernatant or compound
521 solution were deposited on the center of the cotton discs, and the plates were dried for 3
522 min by keeping them completely open in a laminar flow sterile bench. This drying period
523 was done in addition to the regular 20 min drying previously described. 2 µL of an

524 overnight culture of the tested strains were then inoculated at 5 mm from the edge of the
525 cotton discs. The plates were incubated at 30°C for a total of 72 hours. Every 24 hours
526 the cotton discs were reimpregnated with 25 µL of the corresponding supernatant or
527 compound solution. After the incubation period, the plates were used for microscopy
528 analysis without further treatment.

529

530 **Bioassay-guided fractionation.**

531 A 50 mL culture of M5 isolate was grown for 24 h under standard conditions. Bacterial
532 cells were pelleted by centrifugation for 10 min at 6.000 r.c.f. and the supernatant was
533 filtered through a 0.2 µm filter. 25 mL of the supernatant were freeze-dried and the
534 remaining foam was dissolved in 1 mL water. The solution was applied to a Sephadex
535 G20 column (3 cm × 40 cm) and eluted with water collecting 3 mL fractions (50
536 fractions). Fractions were further analyzed using the colony wrinkle formation assay. The
537 fraction with the largest activity was analyzed using an LCMS (Shimadzu Deutschland,
538 Germany) equipped with a Hypercarb column (100 × 3 mm, 3 µM, Thermo Fisher
539 Scientific, flow rate = 0.6 mL min⁻¹, method: 0-10 min: 100% (v/v) water). The main
540 compound of this fraction was purified using a semi-preparative HPLC (Shimadzu
541 Deutschland, Germany) equipped with Hypercarb column (100 × 10 mm, 5 µM, Thermo
542 Fisher Scientific, flow rate = 5 mL min⁻¹, method = 0-20 min: 100% (v/v) water). The pure
543 compound was analyzed using ¹H-NMR spectroscopy, LCMS, and HR-ESIMS. Obtained
544 analytical data were in good agreement with a hypoxanthine standard from Sigma
545 Aldrich.

546

547 **Comparison of hypoxanthine production.**

548 Supernatant of different isolates were heated to 80°C for 15 min and filtered through a
549 0.2 µm syringe filter. The samples were analyzed using an LCMS (Shimadzu
550 Deutschland, Germany) equipped with a Hypercarb column (100 × 3 mm, 3 µM, Thermo
551 Fisher Scientific, flow rate = 0.6 mL min⁻¹, method: 0-10 min: 100% (v/v) water).

552

553 **Cell death assessment.**

554 To visualize cell death in colony biofilms we performed the colony wrinkle formation
555 assay on plates supplemented with 0.25 µM Sytox Green nucleic acid stain (Thermo
556 Fisher Scientific, U.S.A.). After 72 h of incubation, sectors of the colonies that grow
557 around the cotton discs were manually sliced with a scalpel to produce thin cross-
558 sections that include the supporting agar and a sliver of colony biofilm. The cross-
559 sections were placed on a glass slide and used for microscopy without further treatment.
560 All transmitted light and fluorescence images of colony biofilm cross-sections were
561 obtained with an Axio Observer 780 Laser Scanning Confocal Microscope (Carl Zeiss,
562 Germany) equipped with an EC Plan-Neofluar 10x/0.30 M27 objective, an argon laser
563 for stimulation of fluorescence (excitation at 488 nm for green fluorescence and at 561
564 nm for red fluorescence, with emissions at 528/26 nm and 630/32 nm respectively), a
565 halogen HAL-100 lamp for transmitted light microscopy and an AxioCam MRc color
566 camera (Carl Zeiss).

567

568 **Stereomicroscopy and Image Analysis.**

569 All bright-field and fluorescence images of colonies were obtained with an Axio Zoom
570 V16 stereomicroscope (Carl Zeiss, Germany) equipped with a Zeiss CL 9000 LED light
571 source, a PlanApo Z 0.5× objective, HE 38 eGFP filter set (excitation at 470/40 nm and

572 emission at 525/50 nm), HE 63 mRFP filter set (excitation at 572/25 nm and emission at
573 629/62 nm), and AxioCam MRm monochrome camera (Carl Zeiss, Germany).

574

575 Images were obtained with exposure times of 20 ms for bright-field, and 2500 ms for red
576 fluorescence or 3000 ms for green fluorescence when needed. For clarity purposes, the
577 images of colonies are presented here with adjusted contrast and the background has
578 been removed, so that the colony structures can be easily appreciated. The modified
579 pictures were not used for any fluorescence measurements.

580

581 To assess the expression levels of P_{epsA} -*gfp*, P_{tapA} -*gfp*, and $P_{hyperspank}$ -*mKATE*
582 fluorescent reporter fusions in colonies we used ImageJ (National Institutes of Health,
583 USA). Briefly, the average fluorescence emission intensities were measured in the green
584 fluorescence channel for GFP and red fluorescence channel for mKATE by using a
585 region of interest (ROI) that surrounds the cotton discs in the pictures as a partial ring,
586 taking care to avoid the disc area itself. The ROI was drawn in such a way that it avoids
587 the region of the colony that first makes contact with the cotton discs. This ROI had a
588 width of 0.5 mm for measurements done at 40 and 50 hours, and a width of 1 mm for
589 measurements done at 65 hours. The ROI was positioned in each colony image using
590 the bright-field channel, and the average fluorescence intensity was then measured on
591 the corresponding green and red fluorescence images.

592

593 To assess cell death, the average green fluorescence intensity of the cross-sections of
594 colonies treated with Sytox Green was measured. All measurements were done with
595 ImageJ. The colony area was selected on the transmitted light channel of cross-section

596 images using the tracing tool (Legacy mode, tolerance 60). The average fluorescence
597 intensity was then measured in the corresponding areas of the green and red
598 fluorescence channels.

599

600 **Nucleotide sequence accession numbers.**

601 Sequences used in this study have been deposited in GenBank under accession
602 numbers KY705015 (*Lysinibacillus* sp. M2c), KY698015 (*Bacillus pumilus* P22a), and
603 KY703395 (*Acinetobacter variabilis* T7a). Further, the draft genome sequence of *L.*
604 *fusiformis* M5 is available in GenBank under accession number MECQ00000000, and
605 the strain was deposited in the Jena Microbial Resource Collection (ST-Number:
606 ST036146, see <http://www.leibniz-hki.de/en/jena-microbial-resource-collection.html>).

607 **AUTHORS CONTRIBUTIONS**

608 R.G.-M., Á.T.K. conceived the project; R.G.-M., S.K. performed the screen and the
609 microbiology assays; R.G.-M. constructed bacterial strains; S.G., purified hypoxanthine;
610 S.G., R.B., P.S. analyzed the analytical data; R.G.-M., P.S., Á.T.K., wrote and revised
611 the manuscript.

612

613 **ACKNOWLEDGEMENTS**

614 We would like to thank Heike Heineke (HKI Jena) for NMR measurements and Andrea
615 Perner (HKI Jena) for HR-MS measurements.

616 This work received financial support from the Deutsche Forschungsgemeinschaft (DFG)
617 (KO4741/2-1 and KO4741/3-1), from Marie Curie Career Integration Grant

618 (PheHetBacBiofilm), and from the DFG Graduate School Jena School of Microbial

619 Communication (JSMC) (Start-up Grant) to Á.T.K.; from Consejo Nacional de Ciencia y

620 Tecnología, German Academic Exchange Service to R.G.-M.; from the Leibniz

621 Association (Junior Research Group of Pierre Stallforth) to P.S., S.G., R.B; from JSMC

622 (PhD fellowship) to R.B.

623 **REFERENCES**

- 624 1. Hall-Stoodley L, Costerton JW, Stoodley P. 2004. Bacterial biofilms: from the
625 natural environment to infectious diseases. *Nat Rev Microbiol* 2:95–108.
- 626 2. Flemming H-C, Wingender J, Szewzyk U, Steinberg P, Rice SA, Kjelleberg S.
627 2016. Biofilms: an emergent form of bacterial life. *Nat Rev Microbiol* 14:563–575.
- 628 3. West SA, Diggle SP, Buckling A, Gardner A, Griffin AS. 2007. The social lives of
629 microbes. *Annu Rev Ecol Evol Syst* 38:53–77.
- 630 4. Stewart PS, Franklin MJ. 2008. Physiological heterogeneity in biofilms. *Nat Rev*
631 *Microbiol* 6:199–210.
- 632 5. Miquel S, Lagrèfeuille R, Souweine B, Forestier C. 2016. Anti-biofilm activity as a
633 health issue. *Front Microbiol* 7:592. doi: 10.3389/fmicb.2016.00592.
- 634 6. Bjarnsholt T, Alhede M, Alhede M, Eickhardt-Sørensen SR, Moser C, Kühl M,
635 Jensen PØ, Høiby N. 2013. The *in vivo* biofilm. *Trends Microbiol* 21:466–474.
- 636 7. Valderrama WB, Cutter CN. 2013. An ecological perspective of *Listeria*
637 *monocytogenes* biofilms in food processing facilities. *Crit Rev Food Sci Nutr*
638 53:801–817.
- 639 8. Mangwani N, Kumari S, Das S. 2016. Bacterial biofilms and quorum sensing:
640 fidelity in bioremediation technology. *Biotechnol Genet Eng Rev* 8725. doi:
641 10.1080/02648725.2016.1196554.
- 642 9. Ramey BE, Koutsoudis M, Bodman SB Von, Fuqua C. 2004. Biofilm formation in
643 plant-microbe associations. *Curr Opin Microbiol* 7:602–609.
- 644 10. Parsek MR, Greenberg EP. 2005. Sociomicrobiology: the connections between
645 quorum sensing and biofilms. *Trends Microbiol* 13:27–33.
- 646 11. Mhatre E, Monterrosa RG, Kovács ÁT. 2014. From environmental signals to

- 647 regulators: Modulation of biofilm development in Gram-positive bacteria. *J Basic*
648 *Microbiol* 54:616–632.
- 649 12. Espeso DR, Carpio A, Einarsson B. 2015. Differential growth of wrinkled biofilms.
650 *Phys Rev E* 91:22710. doi: 10.1080/02648725.2016.1196554.
- 651 13. Asally M, Kittisopikul M, Rué P, Du Y, Hu Z, Çağatay T, Robinson AB, Lu H,
652 Garcia-Ojalvo J, Süel GM. 2012. Localized cell death focuses mechanical forces
653 during 3D patterning in a biofilm. *Proc Natl Acad Sci U S A* 109:18891–18896.
- 654 14. Wilking JN, Zaburdaev V, De Volder M, Losick R, Brenner MP, Weitz DA. 2013.
655 Liquid transport facilitated by channels in *Bacillus subtilis* biofilms. *Proc Natl Acad*
656 *Sci U S A* 110:848–852.
- 657 15. Vlamakis H, Chai Y, Beaugard P, Losick R, Kolter R. 2013. Sticking together:
658 building a biofilm the *Bacillus subtilis* way. *Nat Rev Microbiol* 11:157–168.
- 659 16. Lopez D, Vlamakis H, Kolter R. 2009. Generation of multiple cell types in *Bacillus*
660 *subtilis*. *FEMS Microbiol Rev* 33:152–163.
- 661 17. Mielich-Süss B, Lopez D. 2015. Molecular mechanisms involved in *Bacillus subtilis*
662 biofilm formation. *Environ Microbiol* 17:555–565.
- 663 18. Kearns DB, Chu F, Branda SS, Kolter R, Losick R. 2005. A master regulator for
664 biofilm formation by *Bacillus subtilis*. *Mol Microbiol* 55:739–749.
- 665 19. Bais HP, Fall R, Vivanco JM. 2004. Biocontrol of *Bacillus subtilis* against infection
666 of Arabidopsis Roots by *Pseudomonas syringae* is facilitated by biofilm formation
667 and surfactin production. *Plant Physiol* 134:307–319.
- 668 20. Chen Y, Yan F, Chai Y, Liu H, Kolter R, Losick R, Guo JH. 2013. Biocontrol of
669 tomato wilt disease by *Bacillus subtilis* isolates from natural environments
670 depends on conserved genes mediating biofilm formation. *Environ Microbiol*

- 671 15:848–864.
- 672 21. Stein T. 2005. *Bacillus subtilis* antibiotics: structures, syntheses and specific
673 functions. *Mol Microbiol* 56:845–857.
- 674 22. Todorova S, Kozhuharova L. 2010. Characteristics and antimicrobial activity of
675 *Bacillus subtilis* strains isolated from soil. *World J Microbiol Biotechnol* 26:1207–
676 1216.
- 677 23. Fernandes PAV, De Arruda IR, Dos Santos AFAB, De Araújo AA, Maior AMS,
678 Ximenes EA. 2007. Antimicrobial activity of surfactants produced by *Bacillus*
679 *subtilis* R14 against multidrug-resistant bacteria. *Brazilian J Microbiol* 38:704–709.
- 680 24. Shank EA, Klepac-Ceraj V, Collado-Torres L, Powers GE, Losick R, Kolter R.
681 2011. Interspecies interactions that result in *Bacillus subtilis* forming biofilms are
682 mediated mainly by members of its own genus. *Proc Natl Acad Sci U S A*
683 108:E1236-1243.
- 684 25. Bleich R, Watrous JD, Dorrestein PC, Bowers AA, Shank EA. 2015. Thiopeptide
685 antibiotics stimulate biofilm formation in *Bacillus subtilis*. *Proc Natl Acad Sci U S A*
686 112:3086–3091.
- 687 26. Powers MJ, Sanabria-Valentín E, Bowers AA, Shank EA. 2015. Inhibition of cell
688 differentiation in *Bacillus subtilis* by *Pseudomonas protegens*. *J Bacteriol*
689 197:2129–2138.
- 690 27. Roesch L, Fulthorpe R, Riva A, Casella G, Hadwin A, Kent A, Daroub S, Camargo
691 F, Farmerie W, Triplett E. 2007. Pyrosequencing enumerates and contrasts soil
692 microbial diversity. *ISME J* 1:283–290.
- 693 28. Fierer N, Lennon JT. 2011. The generation and maintenance of diversity in
694 microbial communities. *Am J Bot* 98:439–448.

- 695 29. Kraemer SA, Kassen R. 2015. Patterns of local adaptation in space and time
696 among soil bacteria. *Am Nat* 185:317–331.
- 697 30. Algburi A, Comito N, Kashtanov D, Dicks LMT, Chikindas ML. 2017. Control of
698 biofilm formation: antibiotics and beyond. *Appl Environ Microbiol* 83:e02508-
699 02516.
- 700 31. Sultana ST, Babauta JT, Beyenal H. 2015. Electrochemical biofilm control: a
701 review. *Biofouling* 31:745–758.
- 702 32. Winkelströter LK, Teixeira FB dos R, Silva EP, Alves VF, De Martinis ECP. 2014.
703 Unraveling microbial biofilms of importance for food microbiology. *Microb Ecol*
704 68:35–46.
- 705 33. Gallegos-Monterrosa R, Mhatre E, Kovács ÁT. 2016. Specific *Bacillus subtilis* 168
706 variants form biofilms on nutrient-rich medium. *Microbiology* 162:1922–1932.
- 707 34. Jiang M, Shao W, Perego M, Hoch JA. 2000. Multiple histidine kinases regulate
708 entry into stationary phase and sporulation in *Bacillus subtilis*. *Mol Microbiol*
709 38:535–542.
- 710 35. Vlamakis H, Aguilar C, Losick R, Kolter R. 2008. Control of cell fate by the
711 formation of an architecturally complex bacterial community. *Genes Dev* 22:945–
712 953.
- 713 36. López D, Kolter R. 2010. Extracellular signals that define distinct and coexisting
714 cell fates in *Bacillus subtilis*. *FEMS Microbiol Rev* 34:134–149.
- 715 37. Roth BL, Poot M, Yue ST, Millard PJ. 1997. Bacterial viability and antibiotic
716 susceptibility testing with SYTOX green nucleic acid stain. *Appl Environ Microbiol*
717 63:2421–2431.
- 718 38. Saxild HE, Nygaard P. 1987. Genetic and physiological characterization of

- 719 *Bacillus subtilis* mutants resistant to purine analogs. J Bacteriol 169:2977–2983.
- 720 39. Michna RH, Zhu B, Mäder U, Stülke J. 2016. SubtiWiki 2.0--an integrated
721 database for the model organism *Bacillus subtilis*. Nucleic Acids Res 44:D654-62.
- 722 40. Murray AW. 1971. The biological significance of purine salvage. Annu Rev
723 Biochem 40:811–826.
- 724 41. Dandanell G, Hove-Jensen B, Willemoës M, Jensen KF. 2008. Nucleotides,
725 nucleosides, and nucleobases. EcoSal Plus 3. doi: 10.1128/ecosalplus.3.6.2.
- 726 42. Torres RJ, Prior C, Garcia MG, Puig JG. 2016. A review of the implication of
727 hypoxanthine excess in the physiopathology of Lesch–Nyhan disease.
728 Nucleosides, Nucleotides and Nucleic Acids 35:507–516.
- 729 43. Kim Y-J, Ryu H-M, Choi J-Y, Cho J-H, Kim C-D, Park S-H, Kim Y-L. 2017.
730 Hypoxanthine causes endothelial dysfunction through oxidative stress-induced
731 apoptosis. Biochem Biophys Res Commun 482:821–827.
- 732 44. Day RO, Kamel B, Kannangara DRW, Williams KM, Graham GG. 2016. Xanthine
733 oxidoreductase and its inhibitors: relevance for gout. Clin Sci 130:2167–2180.
- 734 45. Hill-Perkins M, Jones MD, Karran P. 1986. Site-specific mutagenesis in vivo by
735 single methylated or deaminated purine bases. Mutat Res 162:153–163.
- 736 46. Ayala-García VM, Valenzuela-García LI, Setlow P, Pedraza-Reyes M. 2016. Aag
737 hypoxanthine-DNA glycosylase is synthesized in the forespore compartment and
738 involved in counteracting the genotoxic and mutagenic effects of hypoxanthine
739 and alkylated bases in DNA during *Bacillus subtilis* sporulation. J Bacteriol
740 198:3345–3354.
- 741 47. He M, Li X, Liu H, Miller SJ, Wang G, Rensing C. 2011. Characterization and
742 genomic analysis of a highly chromate resistant and reducing bacterial strain

- 743 *Lysinibacillus fusiformis* ZC1. J Hazard Mater 185:682–688.
- 744 48. Zhao L, Bao G, Geng B, Song J, Li Y. 2015. Draft genome sequence of
745 *Lysinibacillus fusiformis* strain SW-B9, a novel strain for biotransformation of
746 isoeugenol to vanillin. Genome Announc 3:e00289-15.
747 doi:10.1128/genomeA.00289-15.
- 748 49. Gupta S, Goyal R, Nirwan J, Cameotra SS, Tejoprakash N. 2012.
749 Biosequestration, transformation, and volatilization of mercury by *Lysinibacillus*
750 *fusiformis* isolated from industrial effluent. J Microbiol Biotechnol 22:684–689.
- 751 50. Bedrunka P, Graumann PL. 2017. Subcellular clustering of a putative c-di-GMP-
752 dependent exopolysaccharide machinery affecting macro colony architecture in
753 *Bacillus subtilis*. Environ Microbiol Rep. doi:10.1111/1758-2229.12496.
- 754 51. Gallegos-Monterrosa R, Maróti G, Bálint B, Kovács ÁT. 2016. Draft genome
755 sequence of the soil isolate *Lysinibacillus fusiformis* M5, a potential hypoxanthine
756 producer. Genome Announc 4:e01272-16. doi: 10.1128/genomeA.01272-16.
- 757 52. Wang S, Hu A. 2016. Comparative study of spontaneous deamination of adenine
758 and cytosine in unbuffered aqueous solution at room temperature. Chem Phys
759 Lett 653:207–211.
- 760 53. Stefanic P, Decorosi F, Viti C, Petito J, Cohan FM, Mandic-Mulec I. 2012. The
761 quorum sensing diversity within and between ecotypes of *Bacillus subtilis*. Environ
762 Microbiol 14:1378–1389.
- 763 54. Burmølle M, Ren D, Bjarnsholt T, Sørensen SJ. 2014. Interactions in multispecies
764 biofilms: Do they actually matter? Trends Microbiol 22:84–91.
- 765 55. Kobayashi K. 2007. *Bacillus subtilis* pellicle formation proceeds through
766 genetically defined morphological changes. J Bacteriol 189:4920–4931.

- 767 56. Kunst F, Rapoport G. 1995. Salt stress is an environmental signal affecting
768 degradative enzyme synthesis in *Bacillus subtilis*. *J Bacteriol* 177:2403–2407.
- 769 57. Yan X, Yu H-JJ, Hong Q, Li S-PP. 2008. Cre/lox system and PCR-based genome
770 engineering in *Bacillus subtilis*. *Appl Environ Microbiol* 74:5556–5562.
- 771 58. Harwood CR, Cutting SM. 1990. Molecular biological methods for Bacillus. John
772 Wiley & Sons Ltd., Chichester, England.
- 773 59. Devereux R, Wilkinson SS. 2004. Amplification of ribosomal RNA sequences, p.
774 509–522. *In* Kowalchuk, GA, Bruijn, F de, Head, IM, Zijpp, AJ Van der, Elsas, JD
775 van (eds.), *Molecular Microbial Ecology Manual*, 2nd edition. Kluwer Academic
776 Publishers, Dordrecht, The Netherlands.
- 777 60. Zhang Z, Schwartz S, Wagner L, Miller W. 2000. A greedy algorithm for aligning
778 DNA sequences. *J Comput Biol* 7:203–214.
- 779 61. van Gestel J, Weissing FJ, Kuipers OP, Kovács ÁT. 2014. Density of founder cells
780 affects spatial pattern formation and cooperation in *Bacillus subtilis* biofilms. *ISME*
781 *J* 8:2069–2079.
- 782 62. Perego M, Cole SP, Burbulys D, Trach K, Hoch JA. 1989. Characterization of the
783 gene for a protein kinase which phosphorylates the sporulation-regulatory proteins
784 Spo0A and Spo0F of *Bacillus subtilis*. *J Bacteriol* 171:6187–6196.
- 785 63. Wang L, Grau R, Perego M, Hoch JA. 1997. A novel histidine kinase inhibitor
786 regulating development in *Bacillus subtilis*. *Genes Dev* 11:2569–2579.
- 787 64. Grau RR, de Oña P, Kunert M, Leñini C, Gallegos-Monterrosa R, Mhatre E, Vileta
788 D, Donato V, Hölscher T, Boland W, Kuipers OP, Kovács ÁT. 2015. A duo of
789 potassium-responsive histidine kinases govern the multicellular destiny of *Bacillus*
790 *subtilis*. *MBio* 6:e00581-15. doi: 10.1128/mBio.00581-15.

- 791 65. López D, Fischbach MA, Chu F, Losick R, Kolter R. 2009. Structurally diverse
792 natural products that cause potassium leakage trigger multicellularity in *Bacillus*
793 *subtilis*. Proc Natl Acad Sci 106:280–285.
- 794 66. Koo B-M, Kritikos G, Farelli JD, Todor H, Tong K, Kimsey H, Wapinski I, Galardini
795 M, Cabal A, Peters JM, Hachmann A-B, Rudner DZ, Allen KN, Typas A, Gross
796 CA. 2017. Construction and analysis of two genome-scale deletion libraries for
797 *Bacillus subtilis*. Cell Syst 4:291–305.e7.
- 798 67. Murray EJ, Strauch MA, Stanley-Wall NR. 2009. SigmaX is involved in controlling
799 *Bacillus subtilis* biofilm architecture through the AbrB homologue Abh. J Bacteriol
800 191:6822–6832.
- 801 68. Martin M, Dragoš A, Hölscher T, Maróti G, Bálint B, Westermann M, Kovács ÁT.
802 2017. De novo evolved interference competition promotes the spread of biofilm
803 defectors. Nat Commun 8:15127. 10.1038/ncomms15127.
- 804 69. Casadaban MJ, Cohen SN. 1980. Analysis of gene control signals by DNA fusion
805 and cloning in *Escherichia coli*. J Mol Biol 138:179–207.
- 806 70. Kovács ÁT, van Hartskamp M, Kuipers OP, van Kranenburg R. 2010. Genetic tool
807 development for a new host for biotechnology, the thermotolerant bacterium
808 *Bacillus coagulans*. Appl Environ Microbiol 76:4085–4088.
809

810 **FIGURE LEGENDS**

811 Figure 1. Single strain and mixed colonies of *B. subtilis* and selected soil strains. *B.*
812 *subtilis* was differentiated from the soil strains using fluorescence emission (false-
813 colored orange) from a reporter expressed by the P_{hyperspank}-mKATE construct. Colonies
814 are shown after 72 h of incubation. Neighbor colonies were inoculated at 5 mm from
815 each other. Scale bars represent 5 mm.

816

817 Figure 2. Effect of cell-free supernatants of soil strains on the development of *B. subtilis*
818 168 biofilm colonies. Colonies were inoculated with 2 μ L of culture at 5 mm from white
819 cotton discs impregnated with 50 μ L of cell-free supernatant of soil bacteria or 2 \times SG
820 medium. The discs were reimpregnated with 25 μ L of the corresponding medium or
821 supernatant every 24 h. Bright-field images of colonies are shown after 72 h of
822 incubation. The scale bar represents 5 mm.

823

824 Figure 3. Characterization of hypoxanthine standard and cell-free supernatants of *B.*
825 *subtilis* 168 (168), and soil isolates *L. fusiformis* M5 (M5) and *Lysinibacillus* sp. M2c
826 (M2). a) HPLC chromatograms of cell-free supernatants compared to a standard
827 solution of hypoxanthine. b) HPLC chromatogram of *L. fusiformis* M5 cell-free
828 supernatant compared with a standard solution of hypoxanthine, and the *L. fusiformis*
829 M5 cell-free supernatant spiked with a standard of hypoxanthine (M5+). c) ¹H NMR
830 spectrum of isolated hypoxanthine (DMSO-d₆, 600 MHz).

831

832 Figure 4. Effect of cell-free supernatant of *L. fusiformis* M5, guanine, hypoxanthine, and
833 xanthine on the development of biofilm colonies of *B. subtilis* 168 (a) and catabolic

834 pathway of guanine, hypoxanthine and xanthine (b). GuaD: guanine deaminase. Puc:
835 hypoxanthine/xanthine dehydrogenases (PucA-E). Bright-field images of colony areas
836 adjacent to the cotton discs are shown after 72 h of incubation. The scale bar represents
837 5 mm.

838

839 Figure 5. Effect of cell-free supernatant of *L. fusiformis* M5 on the development of biofilm
840 colonies of *B. subtilis* 168 and knock-out mutants of kin-kinase genes. Colonies were
841 inoculated with 2 μ l of culture at 5 mm from white cotton discs impregnated with 50 μ L of
842 cell-free supernatant of *L. fusiformis* M5 or 2 \times SG medium. The discs were
843 reimpregnated with 25 μ L of the corresponding medium or supernatant every 24 h.
844 Bright-field images of colony areas adjacent to the cotton discs are shown after 72 h of
845 incubation. The scale bar represents 5 mm.

846

847 Figure 6. Comparison of fluorescence emission of *B. subtilis* strains carrying the
848 constitutive $P_{hyperspank}$ -*mKATE*, and the P_{epsA} -*gfp* (a-d) or P_{tapA} -*gfp* (e-h), reporter fusions.
849 Bright field (a and e), red fluorescence (b and f), and green fluorescence images (c and
850 g) of representative *B. subtilis* biofilm colonies exposed to cell-free supernatants of *B.*
851 *subtilis* 168, *L. fusiformis* M5 and 2 \times SG medium. Box plots of the ratio of green and red
852 fluorescence emission of biofilm colonies of *B. subtilis* TB869 (d) and TB870 (h)
853 exposed to cell-free supernatants of *B. subtilis* 168, *L. fusiformis* M5 and 2 \times SG medium
854 at different time points. Scale bars represent 5 mm. Box plots (d and h) represent
855 fluorescence ratios of at least 4 independent colonies, processed as described in
856 material and methods. (one-way ANOVA: $P < 0.05$, $n = 4-8$ independent colonies).

857

858 Figure 7. Effect of cell-free supernatant of *L. fusiformis* M5 on the development of
859 colonies of *B. subtilis* 168 knock-out mutants of biofilm matrix biosynthetic operon *epsA*-
860 *O* and *tasA* gene. Colonies were inoculated with 2 μ L of culture at 5 mm from white
861 cotton discs impregnated with 50 μ L of cell-free supernatants of bacterial culture or
862 2 \times SG medium. The discs were reimpregnated with 25 μ L of the corresponding medium
863 or supernatant every 24 h. Bright-field images of colony areas adjacent to the cotton
864 discs are shown after 72 h of incubation. The scale bar represents 5 mm.

865

866 Figure 8. Detection of localized cell death in biofilm colonies of *B. subtilis* exposed to
867 2 \times SG medium (b-e) or cell-free supernatant of *L. fusiformis* M5 (g-j). Schematic
868 representations of the cross-sections are shown from areas adjacent to cotton discs (a
869 and b). Transmitted light (b and g), red fluorescence (c and h), green fluorescence (d
870 and i), and composite images (e and j) of colonies of a *B. subtilis* strain carrying the
871 constitutive $P_{hyperspank}$ -*mKATE* reporter fusion are shown after 72 h of growth on plates
872 with 0.25 μ M of Sytox Green. The brightness and contrasts of the images have been
873 enhanced to facilitate the appreciation of fluorescence signals and colony wrinkles. The
874 scale bars represent 250 μ m.

875

876 Figure 9. Effect of hypoxanthine and cell-free supernatant of *L. fusiformis* M5 on the
877 development of biofilm colonies of *B. subtilis* 168 and knock-out mutants of *pbuO* and
878 *pbuG* permease genes. Colonies were inoculated with 2 μ L of culture at 5 mm from
879 white cotton discs impregnated with 50 μ L cell-free supernatant of *L. fusiformis* M5 or
880 2 \times SG medium. The discs were reimpregnated with 25 μ L of the corresponding medium

881 or supernatant every 24 h. Bright-field images of colony areas close to the cotton discs
882 are shown after 72 h of incubation. The scale bar represents 5 mm.

883 TABLES AND FIGURES

884 Table 1. Strains and plasmids used in this study.

Strain	Characteristics	Reference
<i>B. subtilis</i>		
168	168 1A700 <i>trpC</i> . Jena Stock	(33)
TB48	168 <i>trpC2 amyE::P_{hyperspank}-mKATE (cat)</i>	(61)
JH12638	JH642 <i>trpC2 phe-1 kinA::Tn917(cat)</i>	(62)
JH19980	JH642 <i>trpC2 phe-1 kinB::tet</i>	(63)
RGP0203-4	JH642 <i>kinC::Sp^R</i>	(64)
DL153	NCIB 3610 <i>kinD::tet</i>	(65)
BKE06370	168 <i>trpC2 pbuG::Erm^R</i>	(66)
BKE13530	168 <i>trpC2 kinE::Erm^R</i>	(66)
BKE29990	168 <i>trpC2 pbuO::Erm^R</i>	(66)
NRS2243	NCIB 3610 <i>sacA::P_{epsA}-gfp (neo), hag::cat</i>	(67)
NRS2394	NCIB 3610 <i>sacA::P_{tapA}-gfp (neo)</i>	(67)
Δ <i>eps</i>	168 <i>trpC2 epsA-O::tet</i>	(68)
Δ <i>tasA</i>	168 <i>trpC2 tasA::Km^R</i>	(68)
TB150	168 <i>trpC2 amyE::P_{hyperspank}-mKATE (cat) epsA-O::tet</i>	This study, TB48→ Δ <i>eps</i>
TB171	168 <i>trpC2 amyE::P_{hyperspank}-mKATE (cat) tasA::Km^R</i>	This study, TB48→ Δ <i>tasA</i>
TB812	168 <i>trpC2 amyE::P_{hyperspank}-mKATE (cat) pbuG::Erm^R</i>	This study, BKE06370→TB48
TB813	168 <i>trpC2 amyE::P_{hyperspank}-mKATE (cat) pbuO::Erm^R</i>	This study, BKE29990→TB48
TB822	168 <i>trpC2 amyE::P_{hyperspank}-mKATE (cat) ΔpbuO</i>	This study
TB823	168 <i>trpC2 amyE::P_{hyperspank}-mKATE (cat) ΔpbuO, pbuG::Erm^R</i>	This study, BKE06370→TB822
TB833	168 <i>trpC2 amyE::P_{hyperspank}-mKATE (cat) kinA::Tn917(cat)</i>	This study, JH12638→TB48
TB834	168 <i>trpC2 amyE::P_{hyperspank}-mKATE (cat) kinB::tet</i>	This study, JH19980→TB48
TB835	168 <i>trpC2 amyE::P_{hyperspank}-mKATE (cat) kinC::Sp^R</i>	This study, RGP0203-4→TB48
TB836	168 <i>trpC2 amyE::P_{hyperspank}-mKATE (cat) kinD::tet</i>	This study, DL153→TB48
TB869	168 <i>trpC2 amyE::P_{hyperspank}-mKATE (cat) sacA::P_{epsA}-gfp (neo)</i>	This study, NRS2243→TB48
TB870	168 <i>trpC2 amyE::P_{hyperspank}-mKATE (cat) sacA::P_{tapA}-gfp (neo)</i>	This study, NRS2394→TB48
TB911	168 <i>trpC2 amyE::P_{hyperspank}-mKATE (cat) kinE::Erm^R</i>	This study, BKE013530→TB48
<i>E. coli</i>		

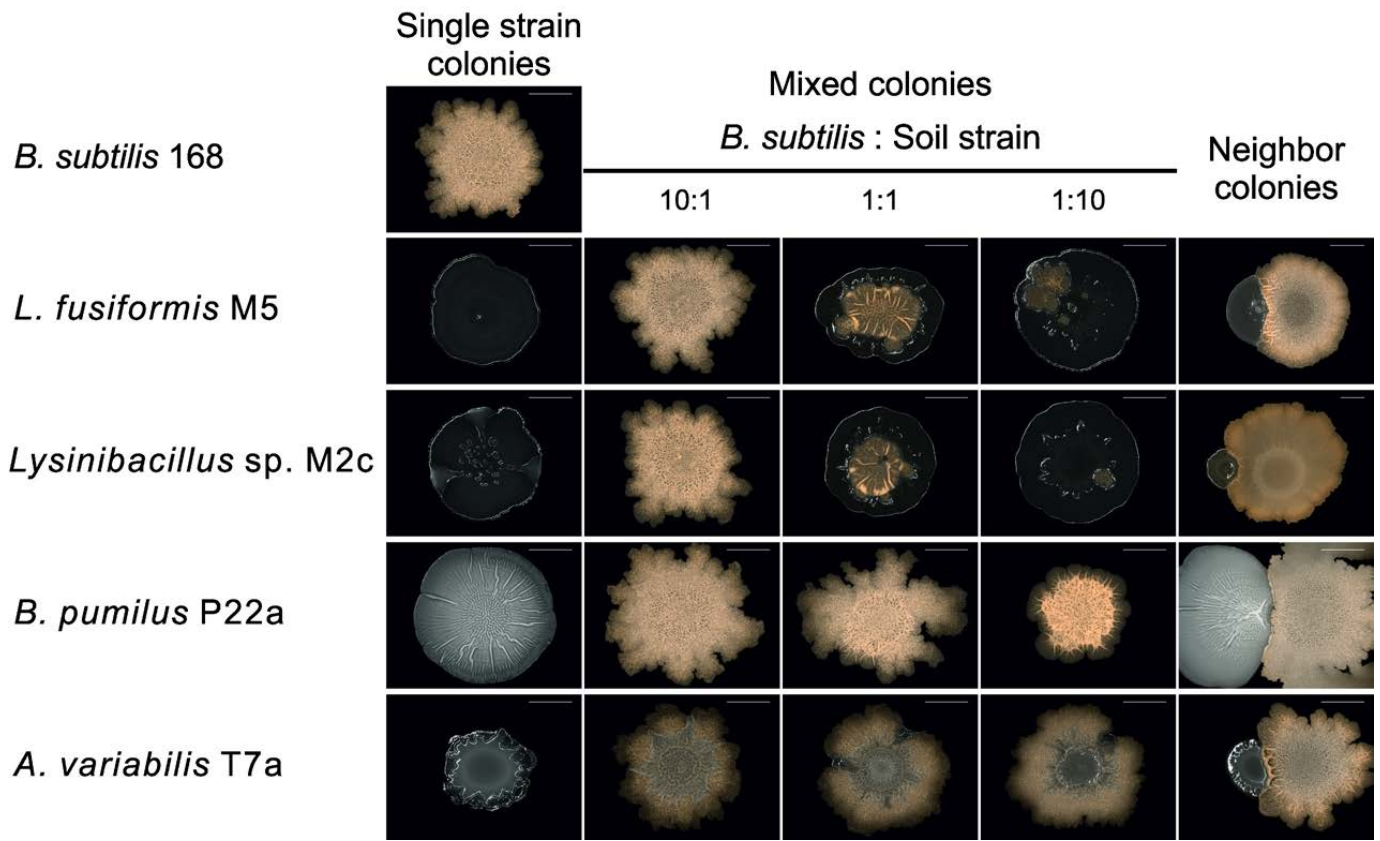
MC1061	Cloning host; K-12 F ⁻ λ ⁻ Δ(<i>ara-leu</i>)7697 [iaraD139]B/r Δ(<i>codB-lacI</i>)3 <i>galK16 galE15 e14⁻ mcrA0 relA1 rpsL150(Str^R) spoT1 mcrB1 hsdR2(r⁻ m⁺)</i>	(69)
Soil Isolates		
<i>Lysinibacillus</i> sp. M2c		This study
<i>Lysinibacillus fusiformis</i> M5		This study
<i>Bacillus pumilus</i> P22a		This study
<i>Acinetobacter variabilis</i> T7a		This study
Plasmid	Characteristics	Reference
pMH66	pNZ124-based Cre-encoding plasmid, Tet ^R Ts	(70)

885

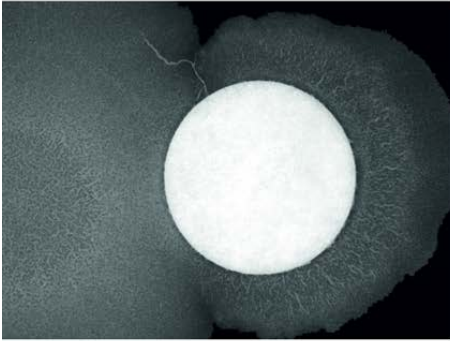
886 Table 2. PCR primers used in this study.

Primer	Sequence (5' → 3')	Target locus
oGFPprev2	TTGTGCCCATTAACATCACC	<i>gfp</i>
oRGM110	GGAATCCGCGCCGTTACATC	<i>pbuG</i>
oRGM111	CAGCCCATATAGCAAAGACC	<i>pbuG</i>
oRGM116	GCGGTGCGGAATAAGTAAAG	<i>pbuO</i>
oRGM117	TACTGAGCGGCACTTGCTTG	<i>pbuO</i>
oRGM130	TATCCACGCCTACGCAGAGC	<i>kinA</i>
oRGM131	CTCAATGGACACGCTGAGAG	<i>kinA</i>
oRGM132	GAAGACCAGCAAAGCAAATCG	<i>kinD</i>
oRGM133	GCGGCTGATCGCCTTTATGG	<i>kinD</i>
oRGM38	GAGAATTCGTGGTGCCAAAGACGAGAAG	<i>tapA</i> promoter
oRGM40	GAGAATTCAGCTGATTAATAGAATAG	<i>epsA</i> promoter
oTB55	CATGGGATCCTGGCGGAGAAGGATTTATG	<i>kinB</i>
oTB56	CACGGAATTCTGTCTCAAACGTGCTCATC	<i>kinB</i>
oTB61	CATGGGATCCATTACGCTAAGCCCTGAG	<i>kinC</i>
oTB62	CACGGAATTCTTGTGCCAGCAAATGATG	<i>kinC</i>
oTB237	TGACGGTAAGGATCGTAG	<i>kinE</i>
oTB238	GTTTCGGCTGTCGTATAG	<i>kinE</i>
27F	AGAGTTTGATCMTGGCTCAG	16S rRNA
1492R	TACGGYTACCTTGTTACGACTT	16S rRNA

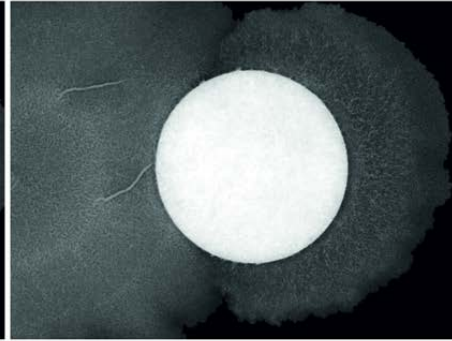
887



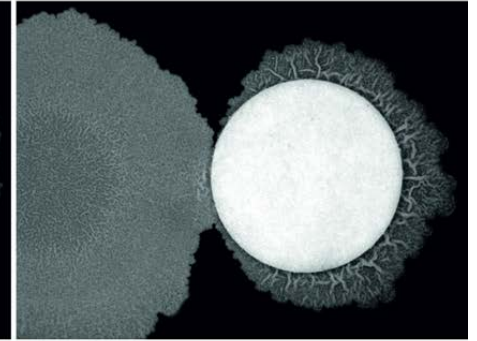
2×SG
medium



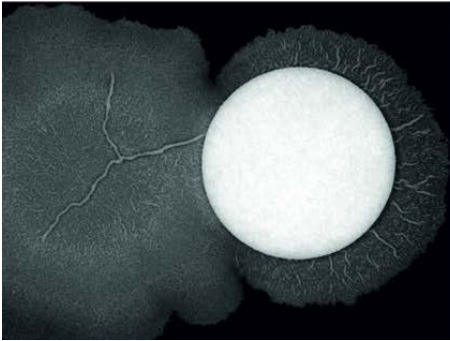
B. subtilis 168
supernatant



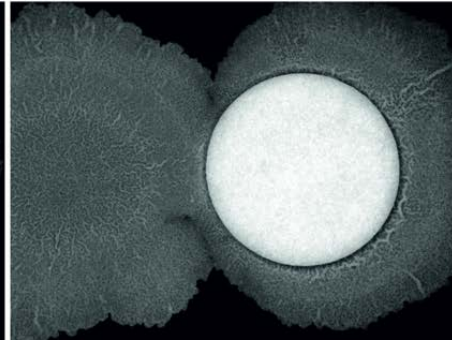
L. fusiformis M5
supernatant



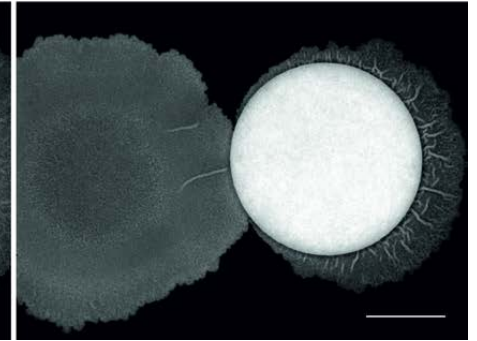
Lysinibacillus sp. M2c
supernatant

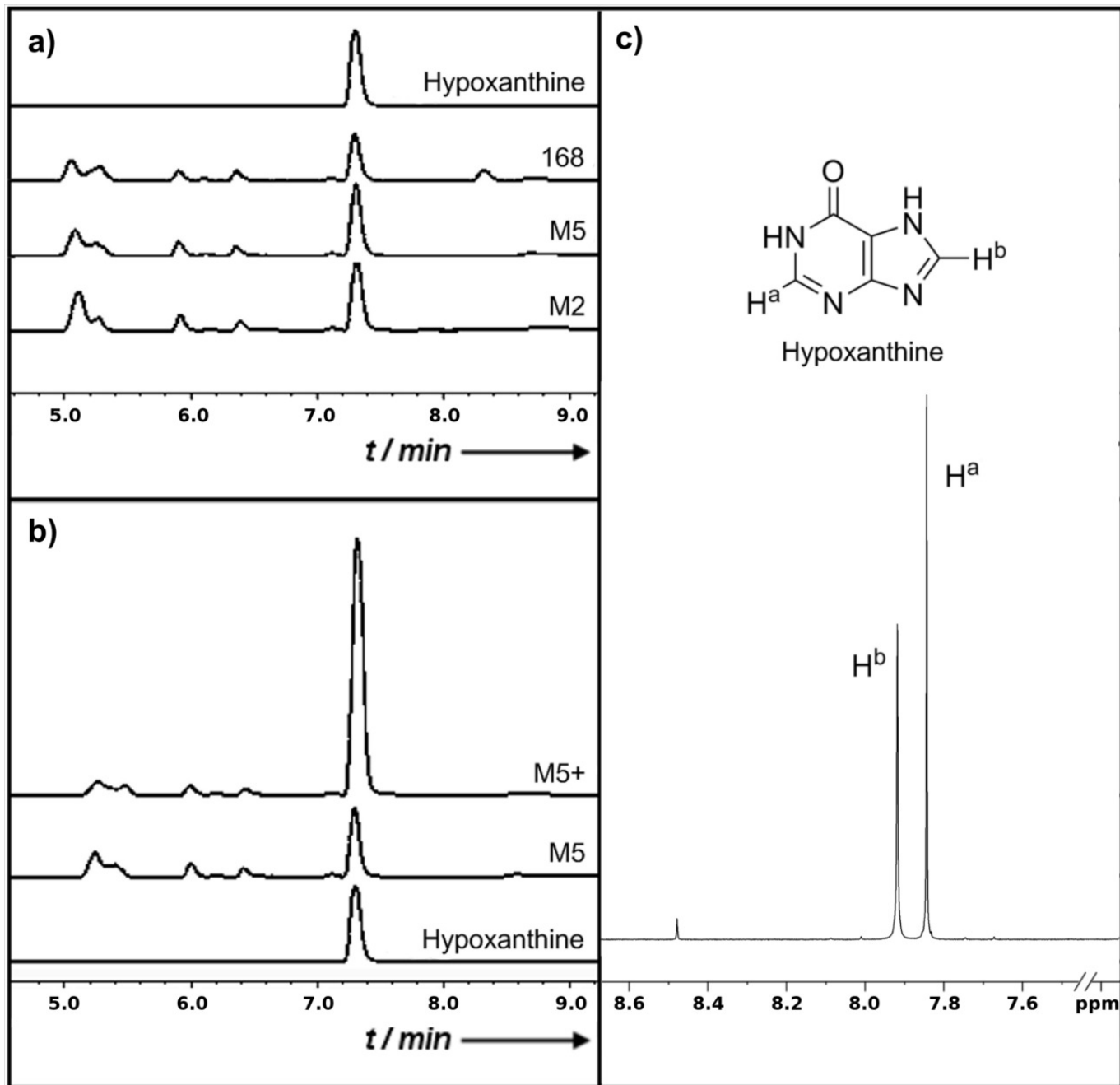


B. pumilus P22a
supernatant

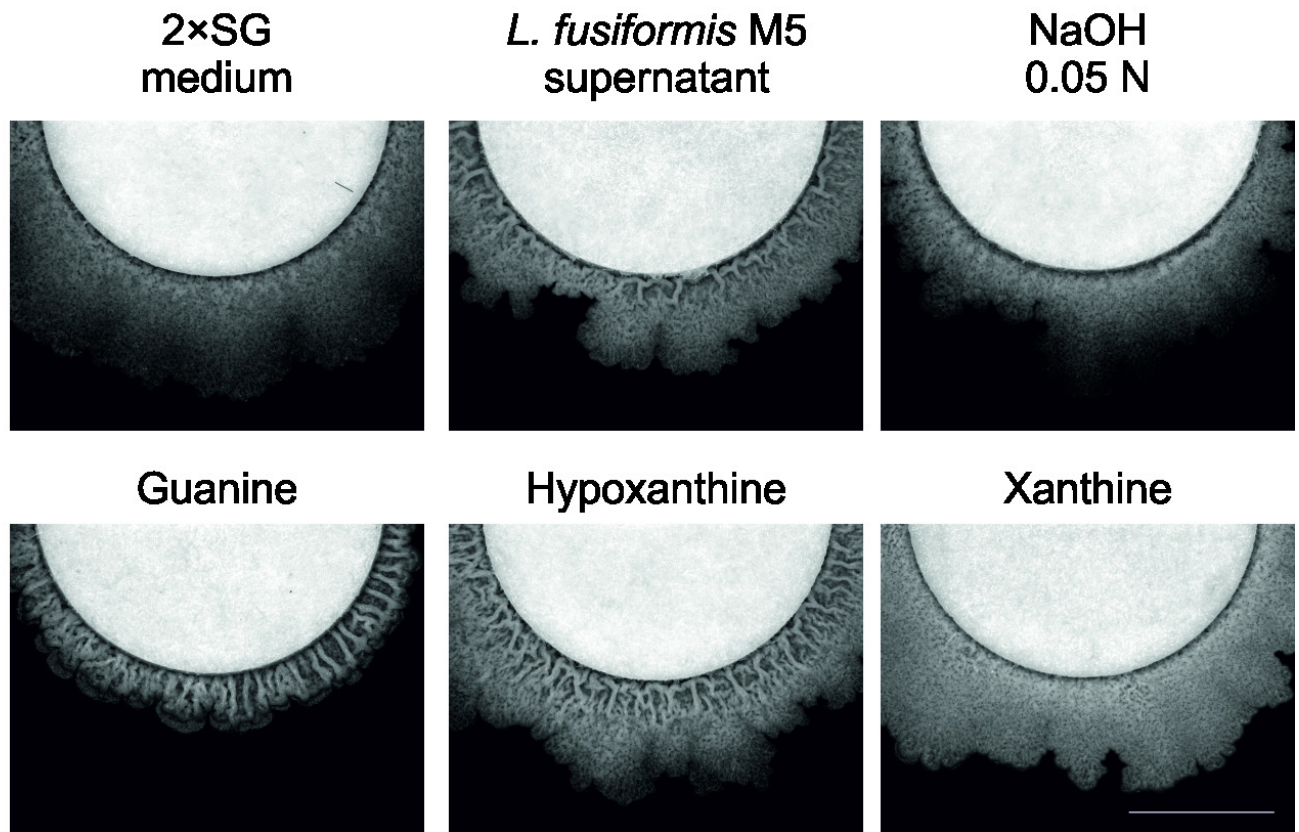


A. variabilis T7a
supernatant

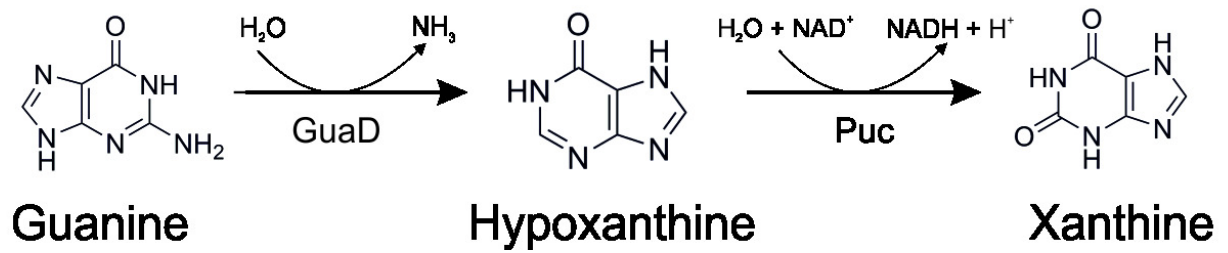


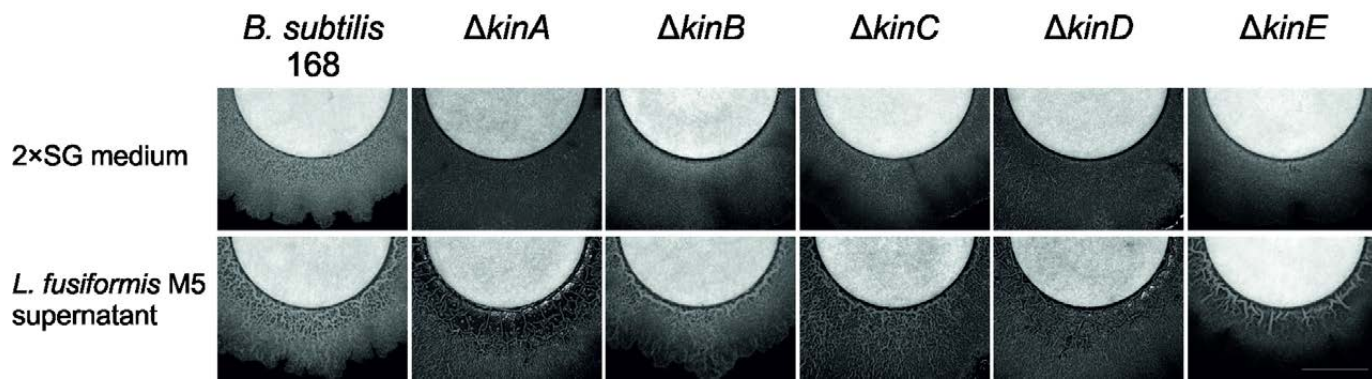


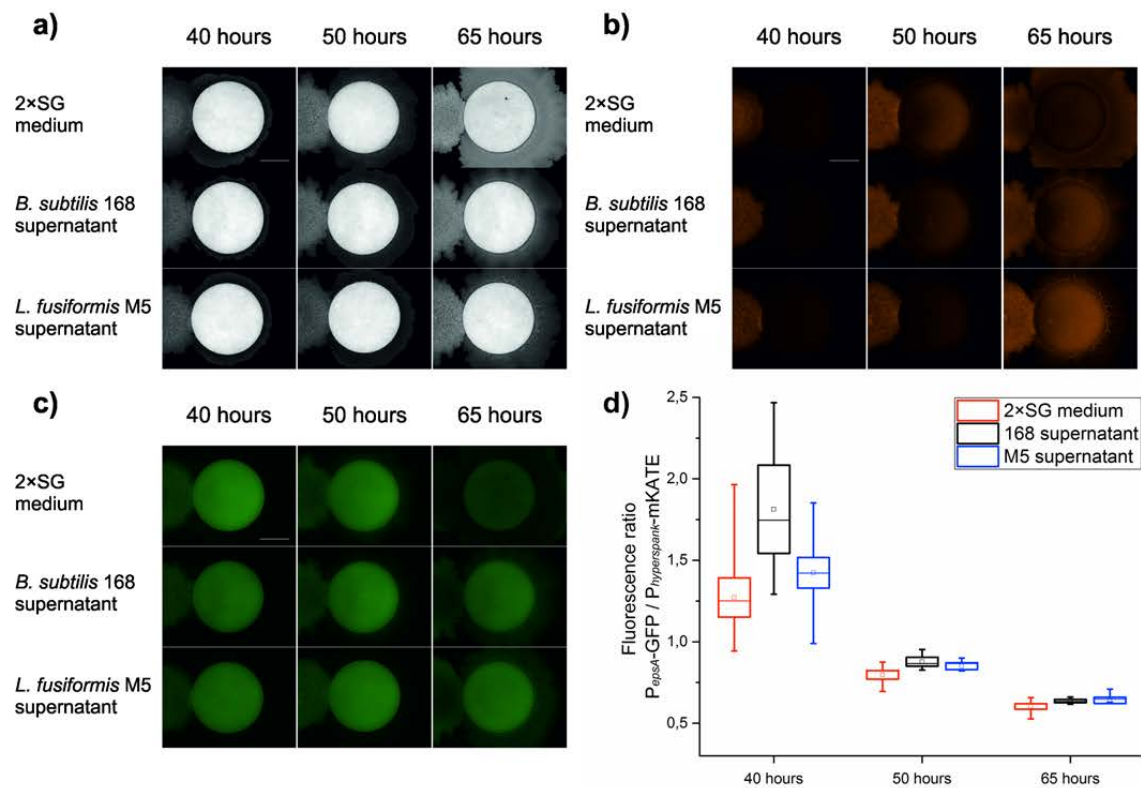
a)



b)





B. subtilis TB869 ($P_{\text{epsA-gfp}}$, $P_{\text{hyperspank-mKATE}}$)*B. subtilis* TB870 ($P_{\text{tapA-gfp}}$, $P_{\text{hyperspank-mKATE}}$)